FEATURES OF THE SURFACE CIRCULATION IN THE NORTHWESTERN JAPAN SEA FROM ERS SYNTHETIC APERTURE RADAR DATA

Dubina V.A., Lobanov V.B., Mitnik L.M.

Pacific Oceanological Institute, Far Eastern Branch, Russian Academy of Sciences, Vladivostok, Russia

Introduction

During two last decades the visible and infrared images from NOAA-series satellites have found extensive applications in studies of water dynamics of the Japan Sea (Huh & Shim, 1987; Isoda & Saitoh, 1993; Isoda, 1994; Ostrovskii, 1993). The NOAA AVHRR images allow the phenomena to be investigated with spatial scales over several kilometers and with temperature contrast of about 0.2 °C against the background. The main attention in these studies was given to the southern Japan Sea including the polar frontal zone (a complex eddy field). Recent researchers began to use the NOAA AVHRR images to study the oceanic dynamics to the north of the polar frontal zone (Ginsburg *et al*., 1998; Goncharenko *et al*., 1993; Kawai & Kawamura, 1997). Cloudiness and weak temperature contrasts in this area render detection of oceanic phenomena impossible. In such conditions, the features of sea surface circulation can be detected by passive and active sensors operating at the microwave range. It was shown that satellite synthetic aperture radar (SAR) has a high potential to study the mesoscale oceanic and atmospheric phenomena (Fu & Holt, 1982; Johannessen *et al*., 1994; Alpers, 1995). These phenomena become visible on SAR images because they are associated with a variable surface currents and variable sea surface wind which modulate the sea surface roughness and thus the normalized radar cross section (NRCS). Increased concentration of surface-active films in the areas with high biological activity is also favorable to the visualization of oceanic dynamic phenomena since the films damp small-scale roughness.

The variations of the NRCS are seen as the brightness variations of SAR image. The eddies, fronts, upwellings, internal waves, and also the diversified atmospheric phenomena are distinguished on SAR images due to their spatial organization. A high spatial resolution of SAR data makes it possible to study sea surface water circulation in a range from hundreds meters to several tens kilometers.

Data

112 ERS-1 and ERS-2 SAR images of the Japan Sea were obtained for performing a project AO3-401: “Mesoscale oceanic and atmospheric phenomena in the coastal area of the Japan and Okhotsk seas: study with ERS SAR and research vessels”, that was selected by the European Space Agency (ESA). The images were acquired in January – December 1991, 1995, and 1997-2000.

The C band SAR operates at a wavelength of 5.6 cm at incidence angle of about 19-26°, has a spatial resolution of about 25 m and a swath width of 100 km.

The imprints of oceanic dynamics were found on about 70% of all images. The following features were revealed:

- *eddies and chains of eddies of different scales, streamers* (SAR images for 22 September 1997; 23 March, 21 April, 7 August and 27 September, 1999, *etc*.);
- *fronts* (SAR image acquired on 16 September 1997);
- *internal waves* (SAR images for 3 and 19 September and 10 October 1997; 27 April and 7 August 1999);
- *upwelling* (SAR image for 16 Sept 1997);
- *river plume* (SAR image for 20 March 1999, *etc*.).

Interpretation of radar signatures was confirmed by their comparison with the NOAA AVHRR visible and IR images, weather maps, bathymetric maps as well as with the hydrographic observations carried out by POI research vessels. The NOAA images were provided by the Institute of Automation and Control Processes, Far Eastern Branch, Russian Academy of Sciences (Vladivostok) and by the Far Eastern Regional Center for Receiving and Processing Satellite Data (Khabarovsk, Russia).

Below three cases are considered. They demonstrate the imprints of the thermodynamic phenomena revealed on the ERS SAR images covering Peter the Great Bay and the areas to the south and to the east of it. The first two cases provide an idea of the eddy structures to the north of 39.5° at the end of cold season and in spring when both the average SST and thermal contrasts increase. The third case demonstrates the potential of the SAR to study upwelling phenomena.

Observation on 23 March 1999

Boundaries of two ERS-2 SAR frames acquired at 13:27 UTC are shown in Fig. 1. They cover coastal mountain area, the Murav'ev-Amursky Peninsula, Vladivostok, Peter the Great Bay and an area south of the bay. Field of sea surface temperature (SST) derived from NOAA AVHRR image (4 channel) visualizes the features of water dynamics in this region at the end of cold season (Fig. 2a). Solid lines in Fig. 2a mark the boundaries of SAR images. Time difference between NOAA AVHRR and ERS-2 SAR images was 7 h and thus the AVHRR data can be used for interpretation of radar signatures.

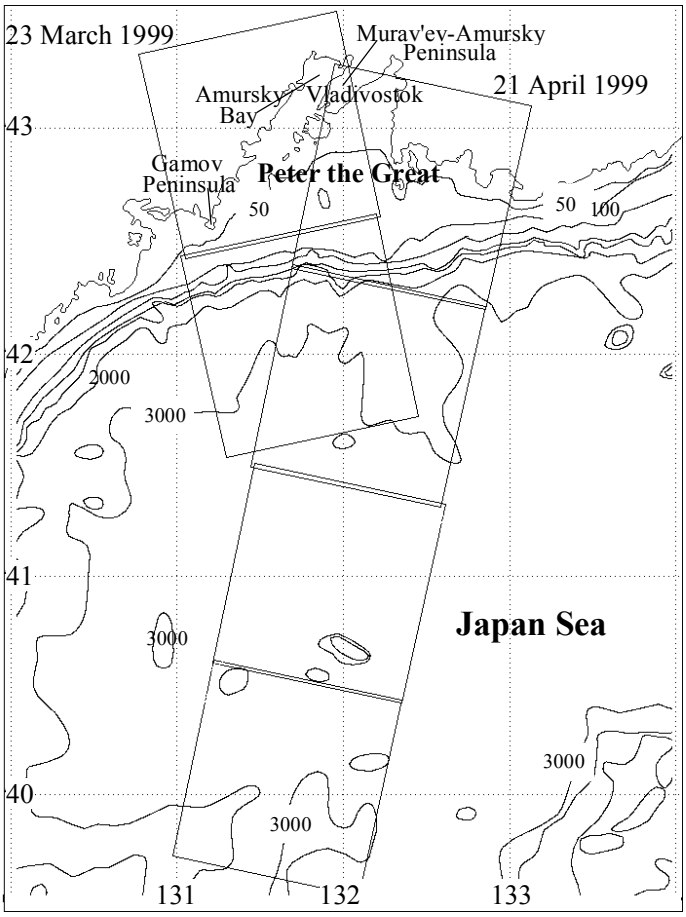

Fig. 1. Bathymetric map of the northwestern Sea of Japan. Rectangles show the boundaries of ERS-2 SAR images acquired on 23 March and 21 April 1999. Line with numbers indicates track and the location of hydrological stations carried out by R/V "Pavel Gordienko" on 18-19 April 1999

On 23 March the northern part of Amur Bay was covered by fast ice. It looks like as a dark-gray area at the top of the bay (Fig. 2b). Large fields of drifting ice II are seen in the middle part of the bay (see interpretation scheme in Fig. 2c that shows the location of contrast details on SAR image). SAR image was obtained at the southern winds of 2-5 m/s that favors to manifestation of the oceanic phenomena on SAR images. The sea areas near the coast where wind speed did not exceed about 3 m/s look dark on the image. Further south at the open sea wind speed is higher. The brightness variations here result mainly from dynamic factors. The most prominent features are three anticyclonic eddies A, B, and ***C*** located at the lower left of the IR image (see an interpretation scheme in Fig. 2c). They are within a SAR swath in full (eddy B) or in part (eddies A and C). The SST decreases from about 1.2 °C at the

center of eddy B to about -0.5°C at its periphery. In the area of eddies A and C the SST is higher and equals to 2.0 °C (Fig. 2a). The values of the NRCS are also higher here compare to the eddy B area (Fig. 2b).

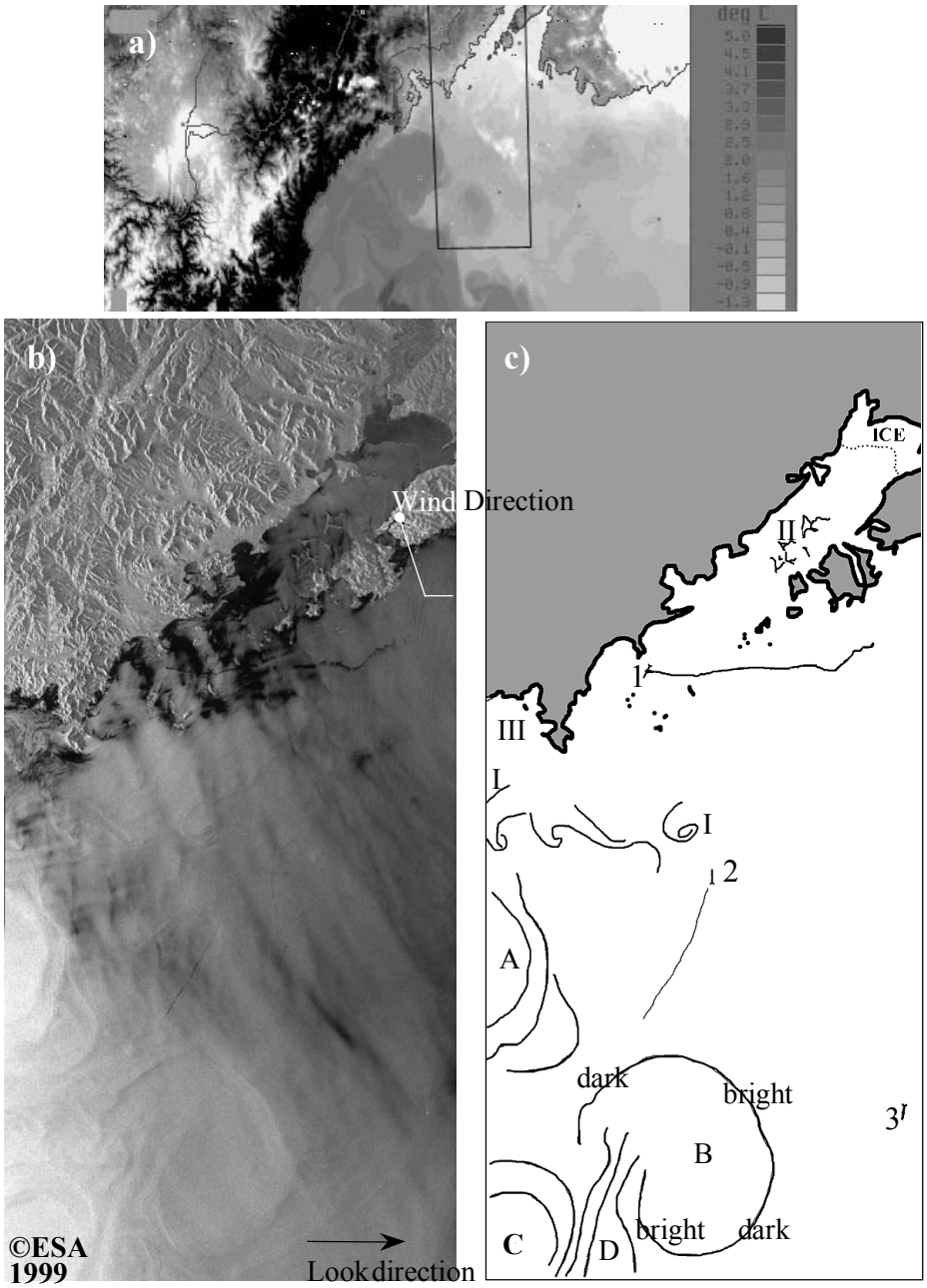

Fig. 2. Manifestations of thermal and dynamic structures on satellite SAR and IR images of the northwestern Japan Sea: a) NOAA AVHRR image acquired on 23 March 1999, at 06:19 UTC. Rectangle indicates the location of the ERS-2 SAR frames; b) ERS-2 SAR image acquired on 23 March 1999, at 13:27 UTC; c) Interpretation scheme showing the location of contrast features on SAR image caused by dynamic factors (chain of eddies formation I-I), thermal and dynamic factors (eddies A, B and C, streamer D), fields of pack ice II, slicks III, and ship wakes 1, 2 and 3, with discharge of polluted water by ships 1 and 2

The presence of a narrow dark band on the upper left and lower right portions of the eddy B, and a bright band on the lower left and upper right corresponds to a typical manifestation of an anticyclonic eddy on a SAR image at the given sounding direction (Johannessen *et al.*, 1996; Lyzenga & Wackerman, 1997). Such signatures are explained by the change of the spectral density of the Bragg waves responsible for backscatter of radar signals. In turn, these changes can result from a variety of physical mechanisms which modulate the sea surface roughness. The main mechanisms are: (a) modulation of the surface wave

spectrum by variable currents (current shift near the boundary of the eddy), (b) variation of the wave spectrum with the change of the relative velocity of wind over the different portions of the eddy (with consideration for azimuthal dependence of the NRCS), and (c) damping of short waves by surface films accumulated by convergent currents.

It follows from a comparison of the SAR (Fig. 2b) and IR (Fig. 2a) images that the SAR image enables one to distinguish the fine details of water dynamics that are not found in SST pattern since their thermal contrasts are weak or absent and their sizes are small. Among these features it should be emphasized a chain of cyclonic eddies I-I the size of about 10 km along a continental slope (see bathymetric contours in Fig. 1), a northward narrow flow of (warmer) water into the anticyclonic vortex B (streamer D), *etc*. The SST values in the area of the eddy chain I-I is about -0.5 °C, and in the streamer D is about 0.8-1.2 °C.

Numbers 1, 2 and 3 in Fig. 2c mark ship wakes. The ships are clearly seen on full-resolution SAR image. Oil-polluted waters behind ships 1 and 2 look dark since oil films also damp small-scale roughness. The area covered by oil film behind ship 1 is about 10 km^2 and the volume of oil in wastewater is about 3 m^3 assuming that an average thickness of the oil film is 0.3 μm.

Observation on 21 April 1999

SAR sensing on 21 April, at 01:58 UTC was also carried out over Peter the Great Bay and the areas south of it (Fig. 3a). Boundaries of the four ERS-2 SAR frames are depicted in Fig. 1. The outlines of radar signatures correlate well with the location of the sharp thermal gradients on NOAA-14 AVHRR image (4 channel) taken four hours later (Fig. 3b). Distributions of water temperature and density deduced from the hydrological measurements carried out by R/V "Pavel Gordienko" on 18-19 April 1999 at stations 33-45 (ship's track and stations' location are shown in Fig. 1) show anticyclonic circulation in the areas A and B and rise of cold water in the area C (Fig. 4). The values of SST reach 6 °C in the anticyclones A and B and decrease to 4°C in the area of cold flow C (Fig. 3b and Fig. 4).

To correlate the SAR signatures with the ship data and SST pattern, a sampling profile in Fig. 3a was taken from point 1 to 2 across areas A, B and C. The profile is shown in Fig. 3c. Its location was close to the ship's track (Fig. 1). To reduce noise the profile is an average of 11 adjacent pixels. The linear increase in counts is due to the decrease of SAR incidence angle from the left to the right side of the image. Positive (a) and negative (b) peaks correspond to crossing of the zones, which are characterized by a large current shift and pronounced thermal gradients. In particular, these zones are observed at the boundaries of the dynamic formations such as eddies, fronts, *etc.*

The areas F near southern Primorye coast are characterized by the low NRCS values (by a dark tone on SAR image) **(**Fig. 3a**)**. They are in a cloudy region on IR-image (Fig. 3b). The appearance of the dark features is likely due to the spring plankton bloom and, hence, increased concentration of natural films, which produce slicks on the sea surface and damp small-scale roughness. The increased concentration of plankton (chlorophyll "a") in the areas under consideration was observed by analysis of satellite ocean color data and was also confirmed by the ship measurements (Shtraihert *et al*., 2000). Slick filaments are visible also in Fig. 2b in the area west of the Gamov Peninsula (area III in Fig. 2c).

Observation on 16 September 1997

Observations carried out on 16 September, at 01:49 UTC over the Japan Sea near Primorye illustrate the manifestations of coastal upwelling on SAR image (Fig. 5a). Coastal mountains are in the upper left of the SAR image. A depth of the sea increases sharply and exceeds 500 m at the distance of about 20-40 km from the coastline. Isobaths from 20 to 3000 m are superimposed on the SAR image.

Appearance of the cold upwelled waters near the southeastern Primorye coast is clearly recognized on NOAA-14 AVHRR image (4 channel) taken on 15 September at 04:37 UTC (Fig. 5b). The cold waters with SST of about 12-13 ℃ are detected in a coastal band of variable width. Two areas with the coldest water where SST drops to 10 ℃ are embedded in the band. Several streamers directed approximately perpendicular to a continental slope transfer the cold coastal waters offshore. A streamer, which is within a SAR swath (solid rectangle in Fig. 5b), has a length of about 100 km and shows anticyclonic circulation.

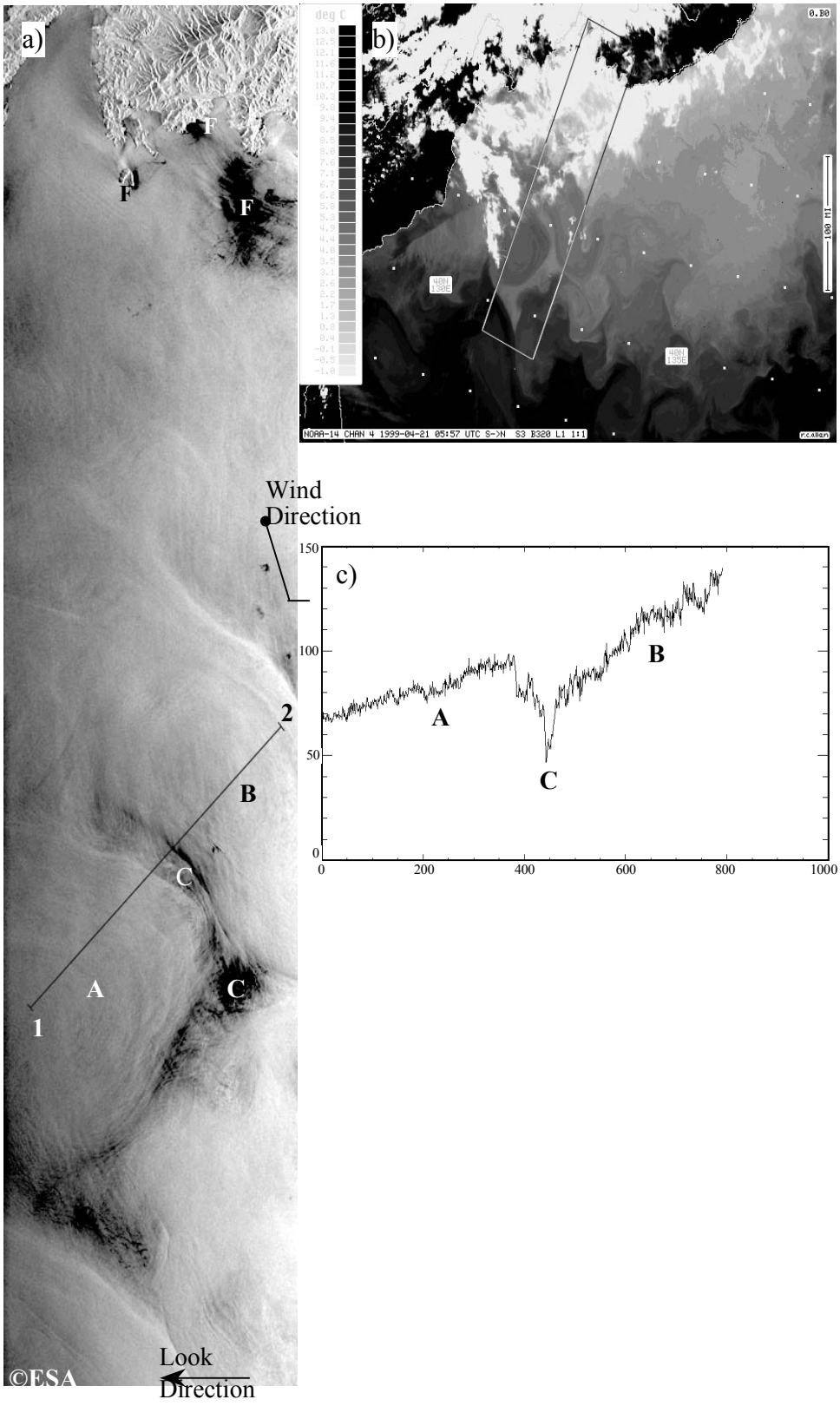

Fig. 3. Satellite SAR and IR images of eddy structures in the northwestern Japan Sea on 21 April 1999: a) ERS-2 SAR image acquired at 01:58 UTC. A and B – anticyclonic eddies, C – areas of colder water, F – areas covered by natural films; b) NOAA AVHRR image acquired at 05:57 UTC. Rectangle indicates the location of the ERS-2 SAR frames; c) Sampling profile of the SAR image between points 1 and 2 across eddy A, an area of cold water C and eddy B

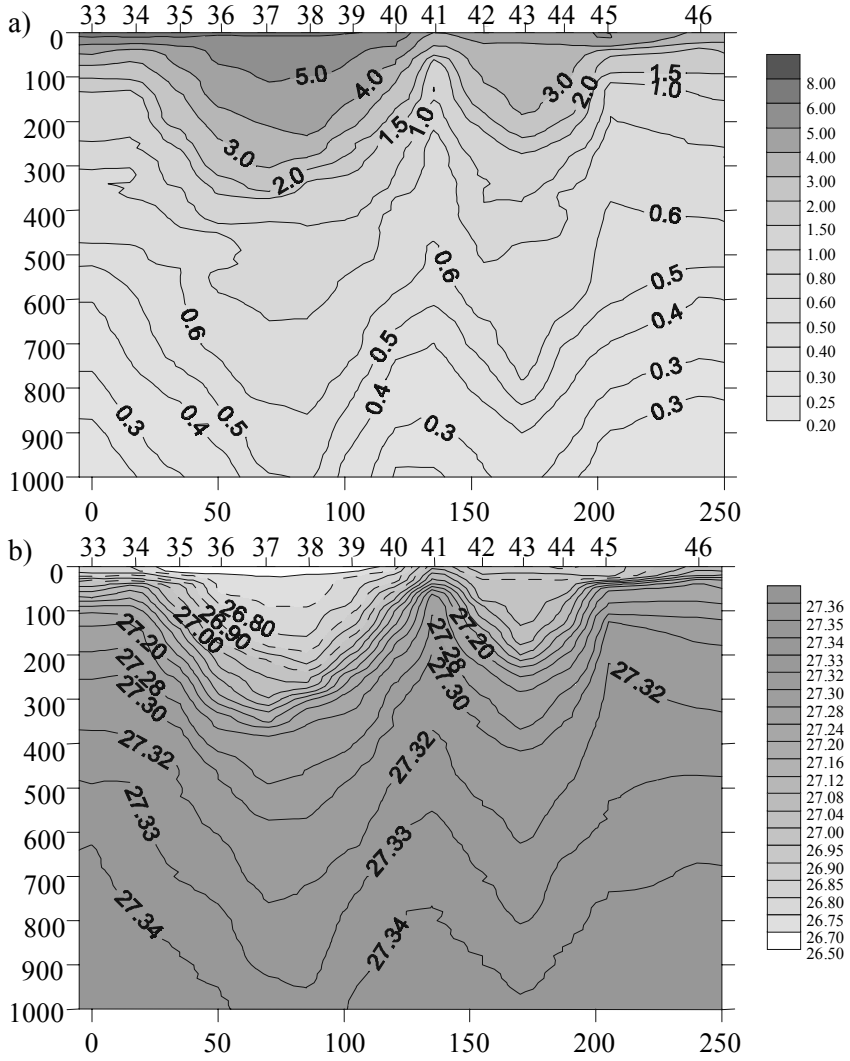

Fig. 4. Distributions of temperature (a) and density (b) of the upper layer (0-1000 dBar) across anticyclonic eddies A and B obtained on 18 April 1999 (R/V "Pavel Gordienko", 32 cruise). Location of hydrological stations is shown in Fig. 1

There are several areas on SAR image that differ in the brightness (NRCS) and in the degree of backscatter homogeneity. Two shore areas 1 (see interpretation scheme in Fig. 5c) are characterized by a darker tone and homogeneous backscatter conditions. These areas agree closely with the area where the SST values are minimal and equal to about 10 °C. The appearance of a bright band A-A (Fig. 5a) is caused by the surface current shift associated with a thermal front near the western boundary of streamer. The area 2 located further offshore where SST is about 14-15 °C looks brighter. Low-contrast regulated structures caused very likely by the organized convection in the marine boundary layer of the atmosphere are visible here. These features are an indicator of the unstable atmospheric conditions when air temperature is below SST. (Air mass, cooled over the cold water, is shifted to the warmer water). The atmosphere becomes still less stable and organized convection more developed over the area 3 south of frontal line B-B, where SST increases to about 17°C. Enhanced brightness of SAR image and much more pronounced inhomogeneity are surface manifestations of this process in a field of sea surface roughness. Similar features were noted also in study of coastal upwelling in the U.S. Mid-Atlantic coastal ocean (Clemente-Colon & Yan, 1999).

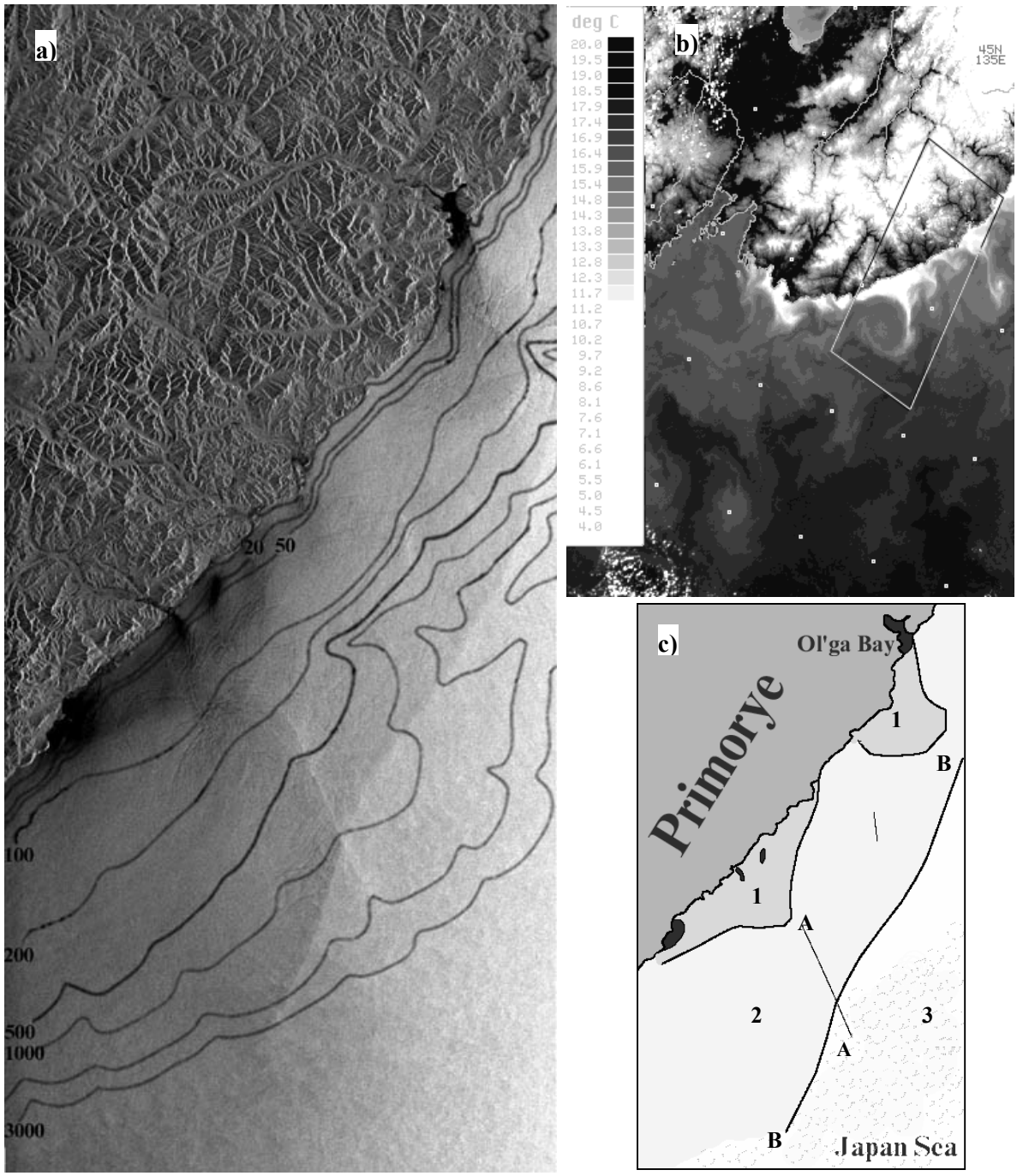

Fig. 5. Surface manifestation of upwelling off the eastern Primorye coast: a) ERS-2 SAR image acquired on 16 September 1997, at 01:49 UTC. Solid lines show bathymetry in meters; b) NOAA AVHRR image acquired on 15 March 1997, at 06:19 UTC. Rectangle indicates the location of the ERS-2 SAR frames; c) Interpretation scheme showing the location of contrast features on SAR image: 1 – the areas of coldest upwelled water, 2 – the area of the water with low temperature, 3 – the area of the warm water with surface manifestation of the organized convection, AA – front line caused by shear of current, BB – thermodynamical frontal line

Conclusion

In this study, ERS-2 SAR images, acquired on 23 March, 21 April 1999 and on 16 September 1999, were processed and interpreted with usage close in time NOAA AVHRR-derived fields of sea surface temperature and ship observations. We analyzed two cases of anticyclonic mesoscale eddy structures south of Peter the Great Bay. Outlines of the mesoscale anticyclonic eddies were similar on SAR and IR images, however, a chain of cyclonic eddies had no thermal manifestation and was detected

by SAR only. We could then show that radar signatures of the anticyclonic eddies were in good agreement with the hydrological measurements carried out by R/V "Pavel Gordienko" and that the alternating dark and bright lines at the eddy boundary correspond to available models. The third case demonstrated that SAR has the potential to detect upwelling phenomena. It was shown that the variations of brightness and structure of different parts of SAR image covering the sea off the Primorye coast correlate well with the SST and that appearance of a cloud-like pattern on SAR image corresponds to the regions with a negative air-sea temperature difference. Such cloud-like signatures are the surface imprints of atmospheric convective cells which form at unstable stratification of the atmosphere.

Acknowledgements

The authors would like to thank the ESA for providing ERS-1/2 SAR data under the ESA AO3-401 (announcement of opportunity) program and the staff of ESRIN for their help in data acquisition. We are grateful to the Institute of Automation and Control Processes (FEB RAS, Vladivostok, Russia) for supplying the NOAA AVHRR data.

References

1. Alpers W. 1995. Measurement of mesoscale oceanic and atmospheric phenomena by ERS-1 SAR // Radio Science Bulletin. N 275. P. 14-22.
2. Clemente-Colon P. & Yan X.-H.. 1999. Observations of East Coast Upwelling Conditions in Synthetic Aperture Radar Imagery // IEEE Trans. Geosci. Remote Sens. Vol. 37. N 5. P. 2239-2248.
3. Fu L.L. & Holt B. 1982. Seasat Views Oceans and Sea Ice with Synthetic Aperture Radar / NASA, JPL Publication. 200 pp.
4. Ginzburg A.I., Kostianoy A.G. & Ostrovskii A.G. 1998. Surface circulation of the Japan Sea (Satellite information and drifters data) // Issledovanie Zemli iz kosmosa. N 1. P. 66-83.
5. Goncharenko I.A., Federyakov V.G., Lasaryuk A.Y. & Ponomarev V.I. 1993. Thematic processing AVHRR data: Study of the coastal upwelling // Issledovanie Zemli iz Kosmosa. N 2. P. 97-107.
6. Huh O.K. & Shim T. 1987. Satellite observations of surface temperatures and flow patterns, sea of Japan and East China Sea, Late March 1979 // Remote Sensing of Environment. Vol. 22. N 5. P. 379-393.
7. Isoda Y. 1994. Warm eddy movements in the Eastern Japan Sea // J. Oceanography. Vol. 50. N 1. P. 1-15.
8. Isoda Y., Saitoh S. 1993. The northward intruding eddy along the east coast of Korea // J. Oceanography. Vol. 49. N 4. P. 443-458.
9. Johannessen J.A., Digranes G., Espedal H., Johannessen O.M., Samuel P., Browne D. & Vachon P. 1994. SAR ocean feature catalogue // ESA Publication SP-1174. ESTEC. The Netherlands. 106 pp.
10. Johannessen J.A., Shuchman R. A., Digranes G., Lyzenga D.R., Wackerman C., Johannessen O.M. P. & Vachon P. W. 1996: Coastal ocean fronts and eddies imaged with ERS 1 synthetic aperture radar // J. Geophysical Research. Vol. 101. N C3. P. 6651-6667.
11. Kawai Y. & Kawamura H. 1997. Characteristics of the satellite – derived sea surface temperature in the oceans around Japan // J. Oceanography. Vol. 53. P. 161-172.
12. Kudryavtcev V.N, Malinovsky V.V. & Rodin A.V. 1999. Manifestations of thermal fronts on the radar images of the ocean // Issledovanie Zemli iz Kosmosa. N 6. P. 16-26.
13. Lyzenga D. & Wackerman C. 1997. Detection and classification of ocean eddies using ERS-1 and aircraft SAR images // Proc. Third ERS Symposium. Florence. Italy. Vol. III. P. 1267-1271.
14. Ostrovskii A.G. 1995. Signatures of stirring and mixing in the Japan Sea surface temperature patterns in autumn 1993 and spring 1994 // Geophysical Research Lett. Vol. 22. N 17. P. 2357-2360.
15. Shtraihert E.A., Alekseev A.V., Vanin N.S., Yurasov G.I. & Zakharkov S.P. 2000. Chlorophyll "a" and the hydrological conditions in Peter the Great Bay in autumn of 1999 // Abstracts CREAMS-2000. Vladivostok. Russia. P. 40.